C.P. No. 657

C.P. No. 657

MINISTRY OF AVIATION

AERONAUTICAL RESEARCH COUNCIL

CURRENT PAPERS

Pressure Measurements on a Cone-Cylinder-Flare Configuration at M=6·85 and Incidences up to 30°

by

D. H. Peckham

LONDON: HER MAJESTY'S STATIONERY OFFICE

1963

PRICE 3s 6d NET

U.D.C. No.533.696.3/.4:533.696.8:533.6.011.55:533.6.013.1:533.6.048.2

C.P. No. 657

January, 1962

PRESSURE MEASUREMENTS ON A CONE-CYLINDER-FLARE CONFIGURATION AT M = 6.85 AND INCIDENCES UP TO 30°

by

D. H. Peckham

SUMMARY

Pressure and force measurements were made on a slender cone-cylinder-flare configuration, slightly blunted at the nose, over an incidence range of 0° to 30° at a Mach number of 6.85.

Although force measurements showed good agreement with Newtonian theory, examination of local pressure distributions revealed considerable departures from theory. Thus it appears that the agreement of force measurements with theory was largely fortuitous, the local errors being self-compensating.

Replaces R.A.E. Tech. Note No. Aero 2806 - A.R.C. 23,691.

LIST OF CONTENTS

LIST OF ILLUSTRATIONS

1 INTRODUCTION

In a recent Note, Woodley[1] reported pressure measurements on a slender cone-cylinder-flare configuration for 0, 3 and 6 degrees incidence. This Note gives results obtained from a similar, but smaller, model which enabled a larger incidence range to be covered, at the expense of fewer pressure-measuring stations and a lower Reynolds number based on model length.

Woodley[1] found that at small angles of incidence, pressures on the conical forebody and conical flare agreed well with the values given in the M.I.T. tables[2] for flow around yawed cones. However, at larger angles of incidence, one has to depend on Newtonian theory and its modifications. In this Note, tests are described which were designed to check the adequacy of Newtonian theory for predicting pressures on slender cone-cylinder-flare shapes at angles of incidence up to 30°.

2 DESCRIPTION OF MODELS AND TESTS

2.1 General

The tests were made in the R.A.E. 7" × 7" hypersonic wind tunnel[3,4] at a Mach number of 6.85, with a stagnation pressure of about 750 p.s.i.g. and a stagnation temperature of approximately 650°K; under these conditions a Reynolds number of 0.5 million per inch is obtained. In order to cover an incidence range up to 30 degrees, while keeping the model in the central core of uniform flow in the working section, it was necessary that the model length be no more than 5 inches, so the Reynolds number based on model length was 2.5 million for the present tests, as compared with about 5 million in the tests reported by Woodley[1]. The geometry of the cone-cylinder-flare is given in Fig.1, with the positions of the pressure holes marked; a separate model was used for force tests. A diagram illustrating the notation used in this Note is given in Fig.2.

2.2 Force measurements

Normal force and pitching moment were measured by means of a simple internal strain gauge balance, with the sting protected from aerodynamic heating by a windshield. Difficulties due to balance heating were anticipated, and since it was desired to avoid the complication of cooling the balance by internal water circulation, the following procedure was adopted. The bridge networks were operated at a nominal 4 volts d.c., and connected to Speedomax recording potentiometers, which have a response time of the order of 1 second for full-scale deflection. The tunnel was started with the model already set at the desired incidence, and after some unsteadiness during the first 1 or 2 seconds of the run due to sting vibration, the readings on the Speedomax recorders settled to a steady value, and the tunnel was shut down after a total running time of about 4 seconds. It was found that a heat pulse, conducted to the upstream end of the balance from the nose of the model, became evident some 5 seconds later, which gave a temperature gradient along the balance and a zero shift. Prior to the next run, the valve connecting the tunnel to the vacuum vessels was closed, and atmospheric air introduced into the working section. This cooled the model and balance to original conditions in a few minutes, when a further run at a new incidence was made. It was not found necessary to re-set zero readings once the balance was cool, and a check calibration of the balance on completion of the tests revealed no change in its properties.

2.3 Pressure measurements

Due to model size limitations, only six $1\frac{1}{2}$ mm O.D. hypodermic pressure tubes could be accommodated, five of these being situated along one generator of the body, with a single hole for checking purposes diametrically opposite

the main pressure hole on the cone forebody (Fig.1). The model could be rotated about its sting support so that pressures at any meridional angle, ϕ, could be measured. The hypodermic pressure tubes were of sufficient length to be led through the incidence actuator to the outside of the working section, thus obviating the heating difficulties usually experienced with flexible rubber connections inside the sting support. Pressures were measured on a conventional multi-tube manometer bank, with one tube referred to a Midwood absolute manometer. Steady readings were obtained after some 10-15 seconds running, when the manometer was clamped and the tunnel shut down. Pressures on the model were obtained for the incidence range 0 to 30 degrees at 3-degree intervals, and for values of the meridional angle, ϕ, from 0 to 180 degrees at 30-degree intervals.

It is thought that manometer readings were measured to an accuracy of ±0.02 inch Hg, which corresponds to ±0.001 in pressure coefficient, C_p. Errors in setting incidence of 0.2 degrees could amount to a further error in C_p of about ±0.002, to give a possible total direct measuring error of ±0.003 on C_p. At low angles of incidence, with the model still close to the centreline of the working section, the variation of $\frac{1}{2}\rho V^2$ in the region of the model was within ±1%; at larger angles of incidence, when the extremities of the model were more than 1 inch off the centreline, the variation of $\frac{1}{2}\rho V^2$ was within ±2% (Ref.4).

3 DISCUSSION OF RESULTS

3.1 Force measurements

Normal force and centre of pressure position are plotted in Fig.3, and compared with estimates made using Newtonian theory*, and with results of tests on a similar model made in the A.R.D.E. 10 inch hypersonic gun tunnel at a Mach number of 8, with a closed jet nozzle[5]. There is good agreement between the two sets of experimental results and theory, except for some evidence in the present tests of a small rearward shift of centre of pressure position, for values of normal force coefficient greater than about 0.25 (20 degrees incidence).

3.2 Pressure measurements

3.2.1 General

The distribution of load along the body is plotted in Fig.4, and was obtained as follows: the pressure distributions at various cross-sections on the cone, cylinder and flare (Figs.5-8), were integrated to give local normal force coefficients, $C_N(x)$, (e.g. Fig.9), these coefficients then being weighted by the local radius of the body, r, to give the local load.

Thus

$$C_N(x) = \int_0^1 \Delta C_p \, d\left(\frac{Y}{r}\right)$$

*Pressure coefficient, $C_p = 2 \sin^2\eta$, where η is the surface incidence at a particular point (i.e. $90^\circ - \eta$ is the angle between the surface normal and the free stream direction, as shown in Fig.2).

where

$$\Delta C_p = (C_p)_\phi - (C_p)_{\pi-\phi}$$

$$\text{Local load} = C_N(x) \cdot \frac{r}{r_c}$$

$$\text{Overall normal force } (C_N)_P = \frac{2\ell r_c}{S} \int_0^1 C_N(x) \frac{r}{r_c} \cdot d\left(\frac{x}{\ell}\right)$$

In Fig.4 it can be seen that Newtonian theory apparently:-

(i) Slightly underestimates the load on the cone forebody at incidences of 12 degrees and more.

(ii) Underestimates the load on the cylindrical section of the body at low angles of incidence, overestimates at high angles of incidence.

(iii) Does not predict the steep rise in load on the flare.

It is unfortunate that there were an insufficient number of pressure holes in the model to enable a more accurate picture of the load distribution to be obtained, but nevertheless it can be seen in Fig.4 that despite the departures of local load from values estimated by Newtonian theory, the overall normal force obtained from an integration of this load distribution would not differ greatly from the Newtonian value. Thus it appears that the close agreement between theory and experimental force measurements (Fig.3) is largely fortuitous, and masks significant local variations from theory.

With regard to pitching moment, the cylindrical mid-section of the body plays little part, being symmetrically disposed about the centre of pressure position. At the lower angles of incidence, it can be seen in Fig.4 that the increase of load on the cone and the flare above theoretical values tends to be self-compensating, but that at the higher angles of incidence, the increase of load on the flare is much greater, and this probably accounts for the rearward shift of centre of pressure position found at angles of incidence greater than about 20° in the balance measurements (Fig.3). A study of Figs.5-8 reveals the causes for the discrepancies between theoretical and experimental values of local normal force coefficient which are discussed in detail below.

3.2.2 Cone pressure distribution

Considering first the conical forebody (Fig.5), it is found that Newtonian theory gives a good estimate of the pressures on the windward surface. At the higher angles of incidence, when most of the upper surface (i.e. $90^\circ < \phi < 180^\circ$) of the conical nose is an expansion region*, suctions of the order of $1/3\ C_{p_{VAC}}$ are obtained, where $C_{p_{VAC}} = -2/\gamma M^2$ corresponds to vacuum. This suction is not predicted by Newtonian theory, which takes no account of the flow on those parts of a body shielded from the "impact flow", but when this suction is allowed for the theoretical and experimental results plotted in Figs.4 and 9 are in close agreement.

---

*The boundary of the expansion region can be calculated from the relationship

$$(\cos \phi)_{ER} = -\frac{\tan \varepsilon}{\tan \alpha} .$$

3.2.3 Cylinder pressure distribution

Pressure distributions at one station ($x/\ell = 0.587$) of the cylindrical mid-section of the body are plotted in Fig.6; the pressure distributions measured at two other stations ($x/\ell = 0.483$ and 0.690) were found to be similar, and the following argument applies, in general, to all three stations. Pressures on the most windward generator ($\phi = 0^{\circ}$) were found to be some 20% less than that predicted by Newtonian theory, but when these values were scaled down in the ratio $C_{p_{\phi=0}}/2 \sin^2\alpha$ ($\simeq 0.8$), it was found that the shapes of the experimental and theoretical pressure distributions were similar on the windward side of the cylinder. For a blunt body with a detached shock, a modified form of Newtonian theory is often preferred, with $C_p = \frac{(\gamma+3)}{(\gamma+1)} \sin^2\eta$, i.e. $C_p = 1.83 \sin^2\eta$ for $\gamma = 1.4$; this expression should be applicable to the case of a cylinder at high incidence when the shock is parallel to the body surface (as in Fig.10), but even using this modified form, the pressures on the windward generator are still about 10% below theory. Over most of the upper surface of the cylinder, suctions of the order of $1/2\ C_{p_{VAC}}$ are attained at incidences of 12 degrees and more. This suction amounts to a significant proportion of the local normal force at the lower angles of incidence, and accounts for the apparent underestimate of load at these incidences in Fig.4, where only forces arising from "impact flow" were considered; at higher Mach numbers, when $C_{p_{VAC}}$ would be less, this effect would be less noticeable.

3.2.4 Flare pressure distribution

Pressure distributions at two stations on the flared afterbody are plotted in Figs.7 and 8 ($x/\ell = 0.794$ and 0.896 respectively); reference to Fig.4 shows that at the first of these stations the local load is below that predicted by Newtonian theory, while at the second station the load is above the Newtonian value. In Fig.7 it can be seen that at the lower angles of incidence the experimental pressures are well below the theoretical values, but that agreement becomes closer as the incidence is increased, while further downstream on the flare (Fig.8), the pressures at the $\phi = 0^{\circ}$ position are consistently about 20% above the Newtonian value, with distortion of the shape of the pressure distribution from the theoretical shape. Examination of the flow photographs in Fig.10 shows that the shock at the cylinder/flare junction is curved, due presumably to a non-uniform flow upstream of the junction, and this is presumably the cause of the non-uniform load on the flare. At the higher angles of incidence, the bow shock wave lies sufficiently close to the body on the windward side to intersect with the flare shock wave in the vicinity of the flare itself. This effect has been noted elsewhere, and was associated with a peak in pressure and heat transfer coefficient. On the leeward side of the flare, suctions of the order of $1/2\ C_{p_{VAC}}$ were attained at incidences of 12° or more, this level being approximately the same as that obtained on the leeward side of the cylindrical mid-section of the body.

It is worth noting that an opposite effect can be obtained with a blunt-nosed flare-stabilised body of revolution. In this case, the blunt bow shock lies further away from the body surface, with the result that the flare is embedded in a low energy stream, with consequent low pressures on the flare.

4 CONCLUSIONS

Although overall force measurements were in good agreement with Newtonian theory, examination in detail of the pressure distributions on the body revealed considerable departures from theory. It would appear, therefore, that the apparent agreement of the force measurements with theory was largely fortuitous through local errors being self-compensating. These tests show the danger, and limited value, of overall force measurements made on their own, since agreement between theory and experiment does not necessarily mean that the type of flow assumed exists in reality.

It is hoped that experiments under way in the R.A.E. hypersonic tunnel[6] will shed further light on these questions.

LIST OF SYMBOLS

x,y,z	rectangular body co-ordinates
ℓ	model length
p	surface pressure on body
p_∞	free stream static pressure
r	local body radius
r_c	radius of cylindrical mid-section of body
M	free stream Mach number
S	model plan area
V	free stream velocity
α	angle of incidence (degrees)
γ	ratio of specific heats for air (= 1.4)
ε	semi-angle of cone forebody and conical flare
ϕ	meridional angle measured in the y z plane of the body, relative to the most windward generator
η	surface incidence at a particular point (i.e. $90^\circ-\eta$ is the angle between the surface normal and the free stream direction)
C_N	overall normal force coefficient
$C_N(x)$	local normal force coefficient
C_p	surface pressure coefficient $\left(= \dfrac{p-p_\infty}{\gamma/2\ p_\infty M^2}\right)$

Suffixes

B	model base area
P	model plan area

LIST OF REFERENCES

Ref. No.	Author	Title etc.
1	Woodley, J.G.	Pressure measurements on a cone-cylinder-flare configuration at small incidences for M = 6.8. A.R.C. C.P.632, March, 1961.
2	Kopal, Z. (Ed.)	Tables of supersonic flow around yawing cones. M.I.T. Center of Analysis Technical Report No.3. 1947.
3	Crabtree, L.F. Crane, J.F.W.	The 7 in. x 7 in. hypersonic wind tunnel at R.A.E./Farnborough. Part 1. Design, instrumentation and flow visualisation techniques. A.R.C. C.P.590, August, 1961.
4	Crane, J.F.W.	The 7 in. x 7 in. hypersonic wind tunnel at R.A.E./Farnborough. Part 2. Heater performance. Part 3. Calibration of the flow in the working section. A.R.C. C.P.590, August, 1961.
5	Cable, A.J. Bowman, J.E.	Hypersonic wind tunnel measurements of the normal forces and centres of pressure of three cone-cylinder-flare models. R.A.R.D.E. Memo (B) 19/62 A.R.C.23,825, May, 1962.
6	Peckham, D.H.	A proposed programme of wind tunnel tests at hypersonic speeds to investigate the lifting properties of geometrically slender shapes. R.A.E. Technical Note No. Aero 2730, A.R.C.22,594, December, 1960.

WT.2078 C.P.657 K3. Printed in England.

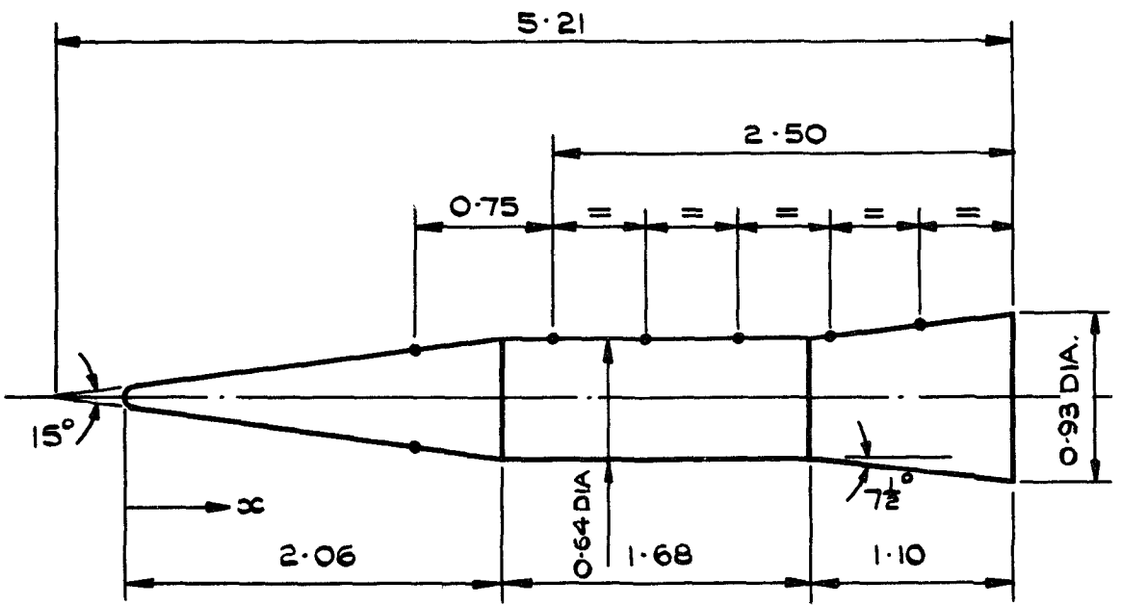

FIG. 1. SKETCH OF MODEL SHOWING POSITIONS OF PRESSURE HOLES.

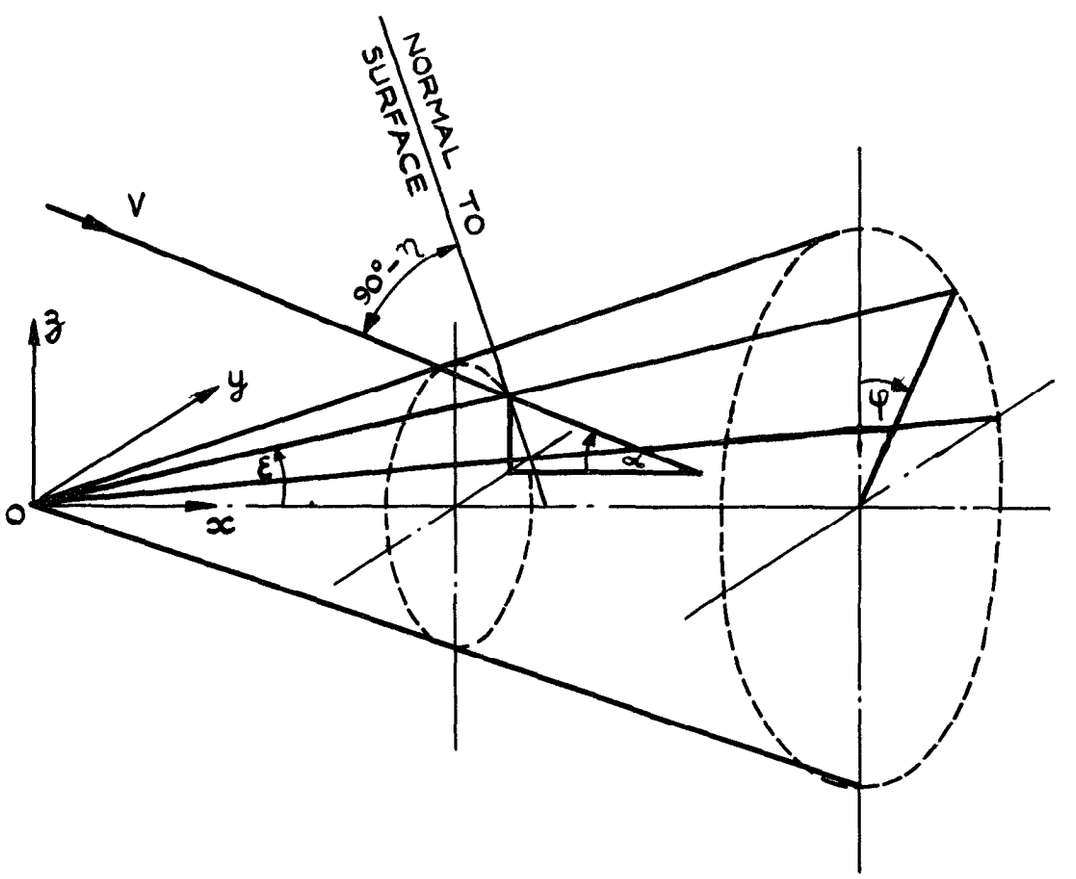

FIG. 2. NOTATION.

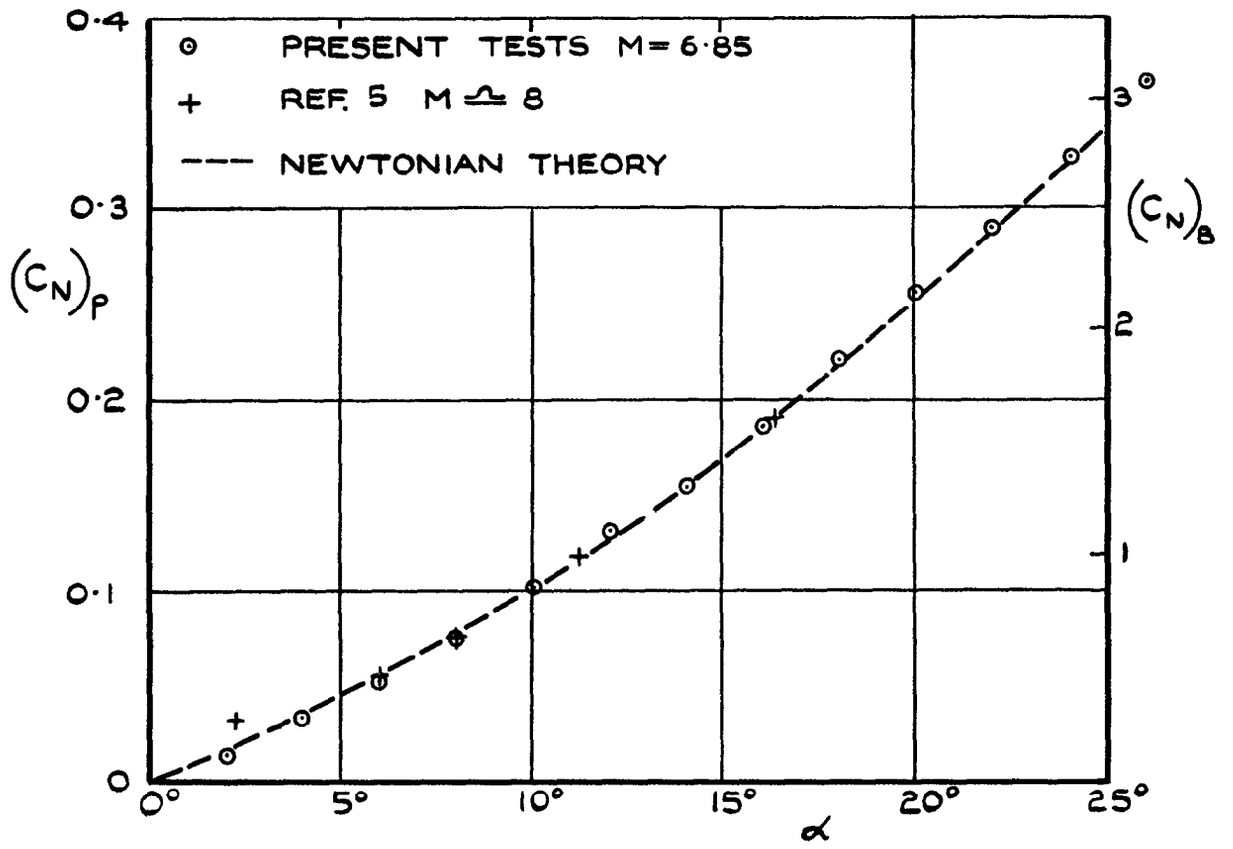

(a). NORMAL FORCE.

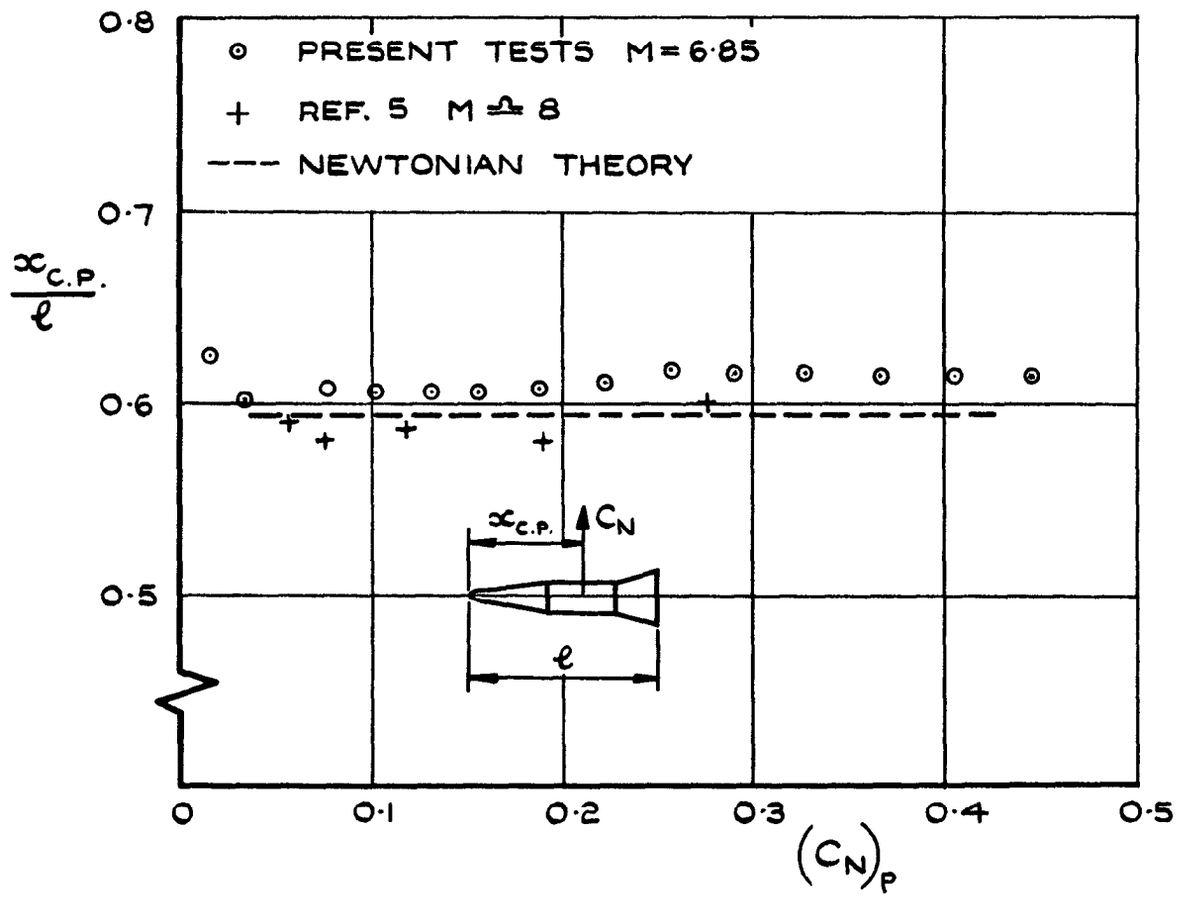

(b). CENTRE OF PRESSURE POSITION.

FIG. 3. NORMAL FORCE AND CENTRE OF PRESSURE POSITION FROM BALANCE MEASUREMENTS.

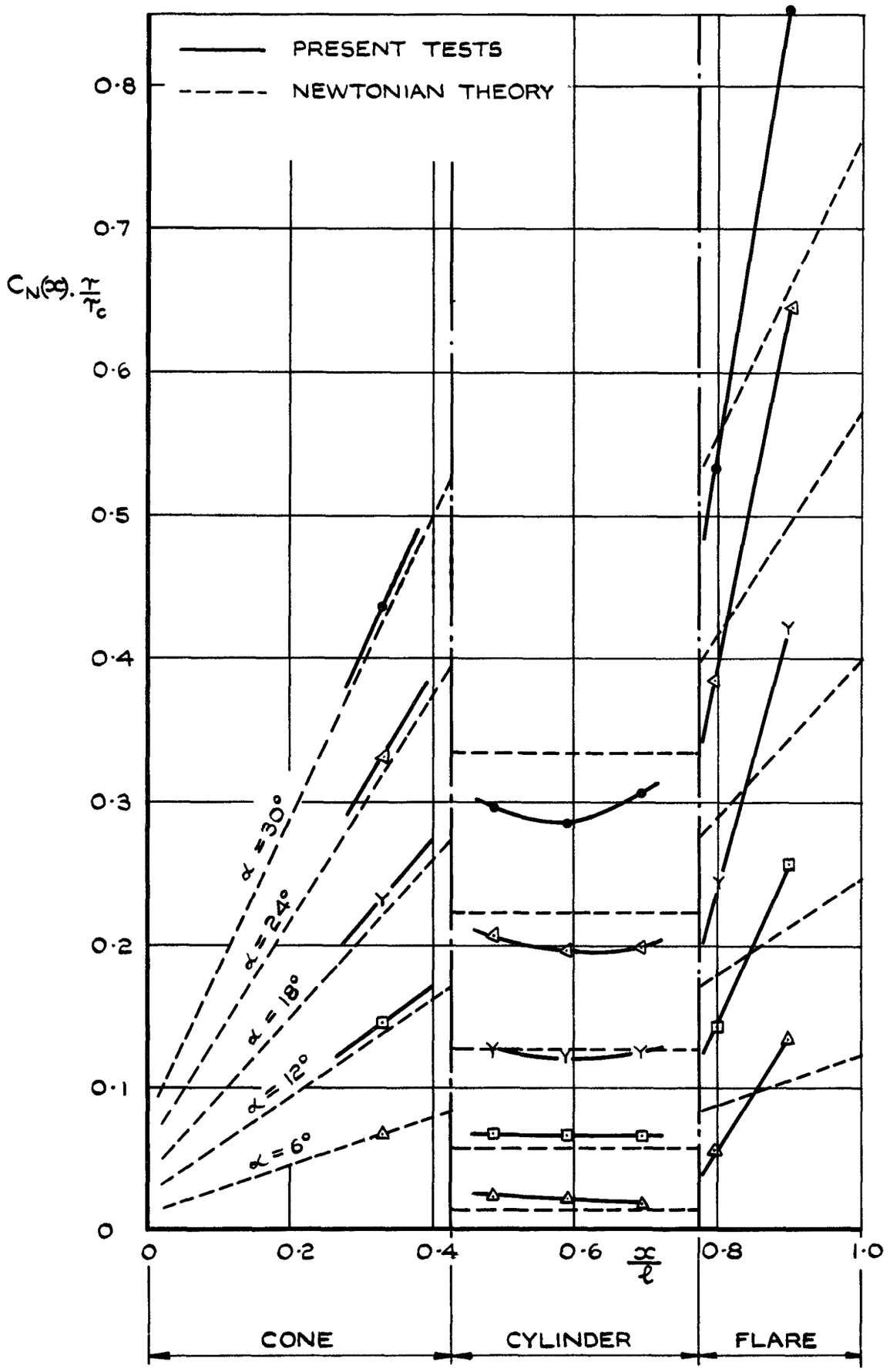

FIG. 4. LONGITUDINAL DISTRIBUTION OF LOAD.

$$C_N(x) = \int_0^{} \Delta C_p \, d\left(y/r\right) \quad \text{WHERE} \quad \Delta C_p = (C_p)_\varphi - (C_p)_{\pi-\varphi}$$

$$\text{OVERALL NORMAL FORCE,} \quad (C_N)_p = \frac{2\ell r_c}{S} \int_0^{} C_N(x) \cdot \frac{r}{r_c} \cdot d\left(x/\ell\right).$$

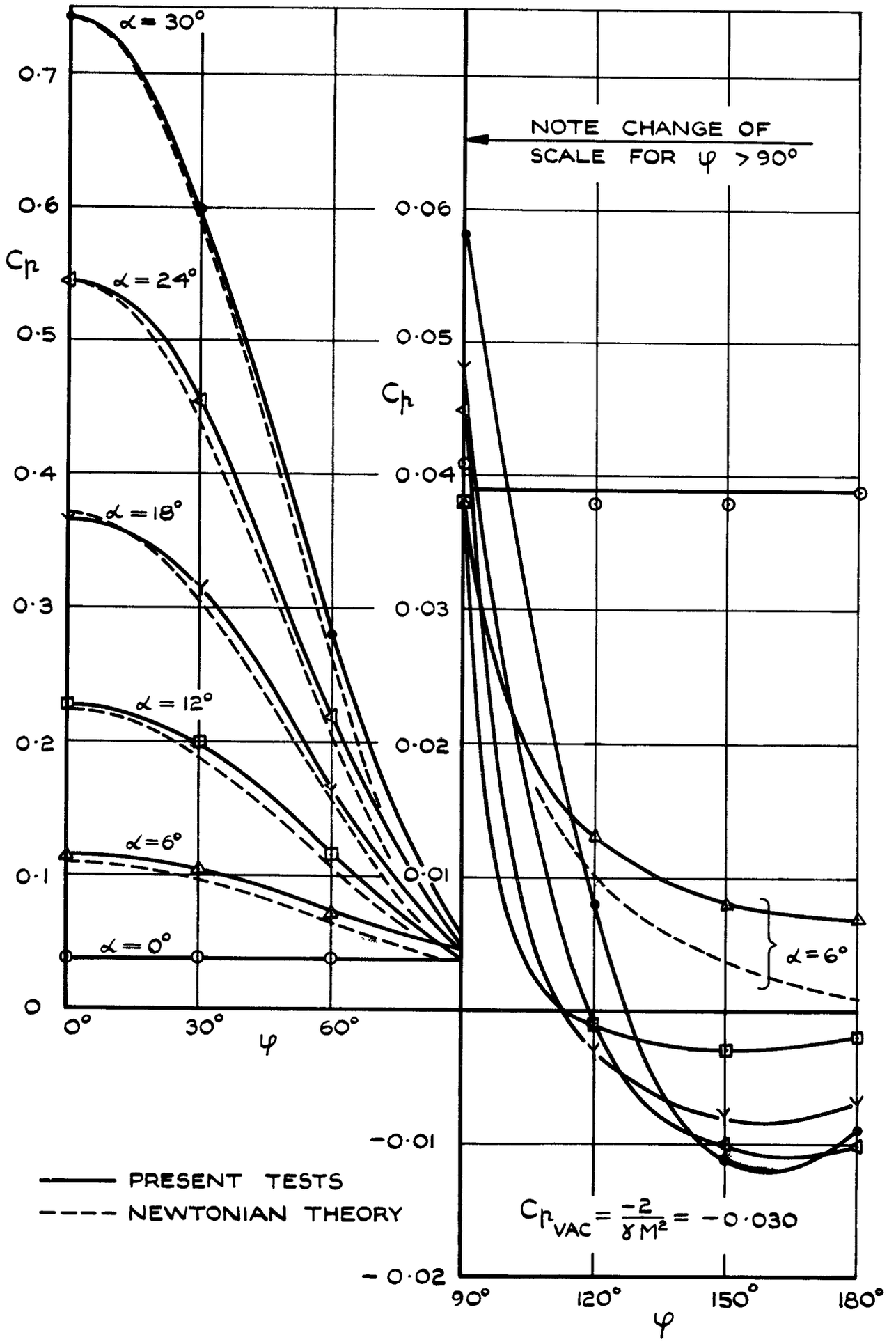

FIG. 5. VARIATION OF C_p ON CONE FOREBODY WITH INCIDENCE & MERIDIAN ANGLE. $\frac{x_s}{\ell} = 0.328$.

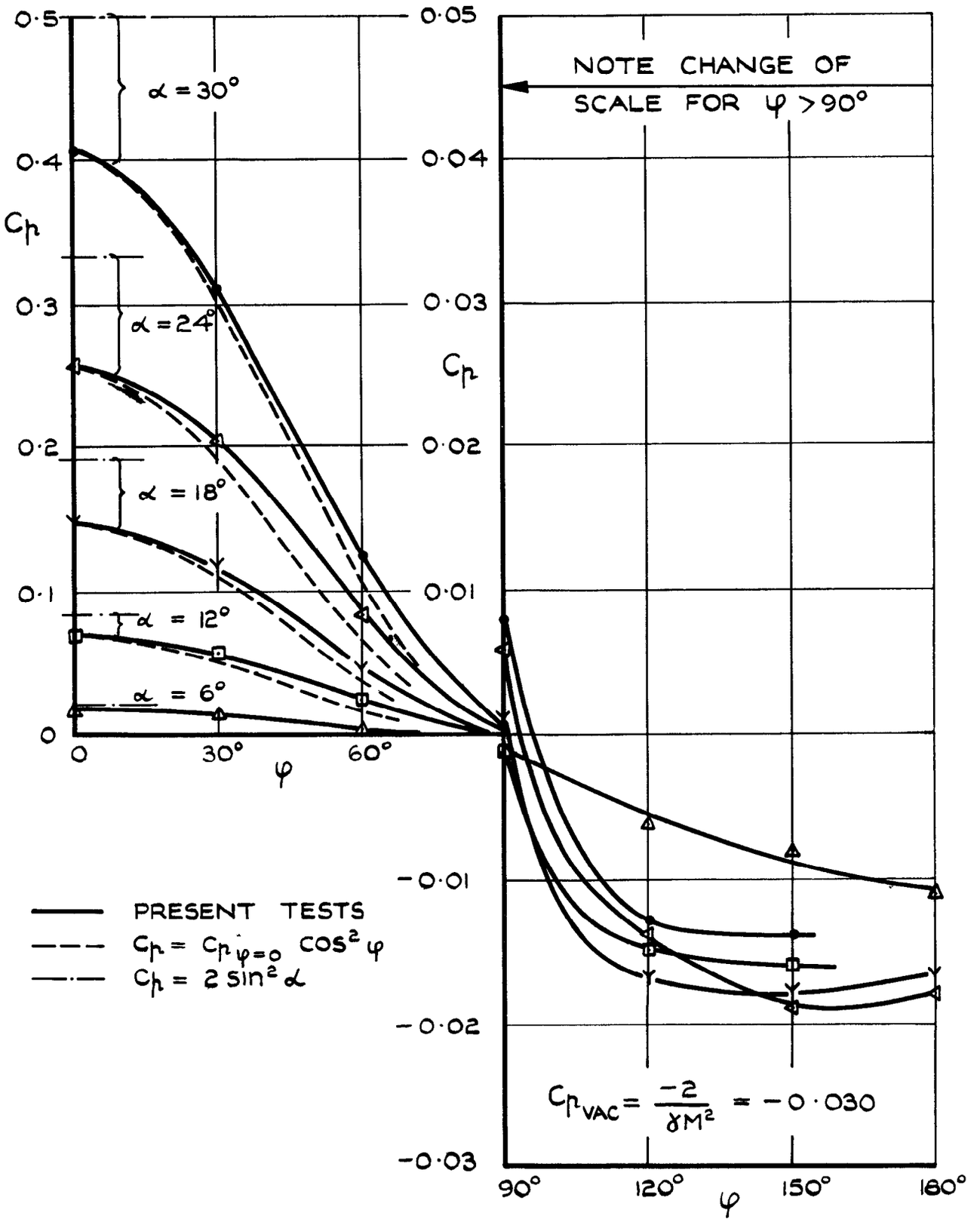

FIG. 6. VARIATION OF C_p ON CYLINDER MID-SECTION WITH INCIDENCE AND MERIDIAN ANGLE. $\frac{x}{\ell} = 0·587$.

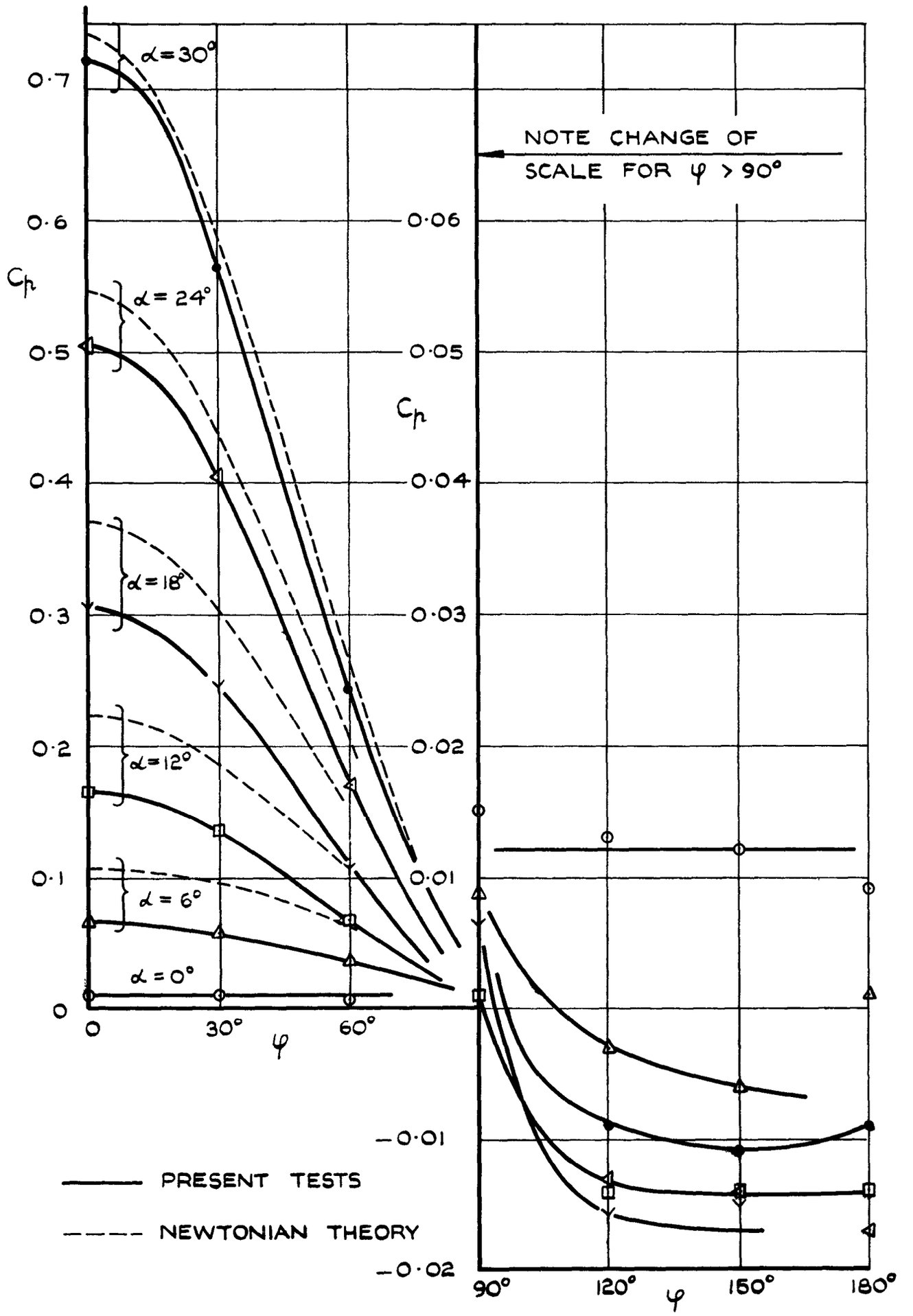

FIG. 7. VARIATION OF C_h ON FLARE AFTERBODY. WITH INCIDENCE & MERIDIAN ANGLE. $\frac{x}{\ell} = 0{\cdot}794$.

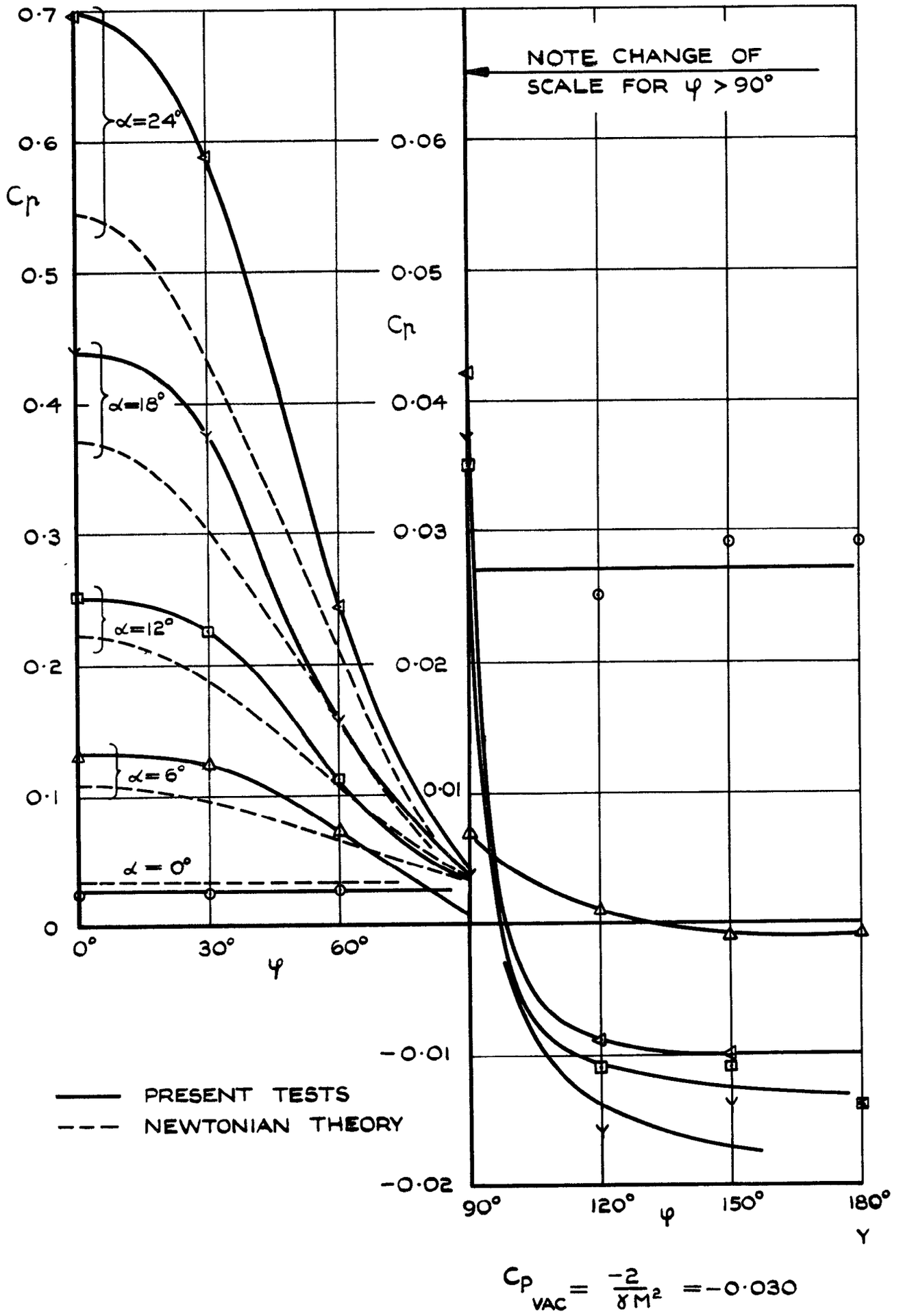

FIG. 8. VARIATION OF C_p ON FLARE AFTERBODY WITH INCIDENCE & MERIDIAN ANGLE. $\frac{x_c}{\ell} = 0.896$.

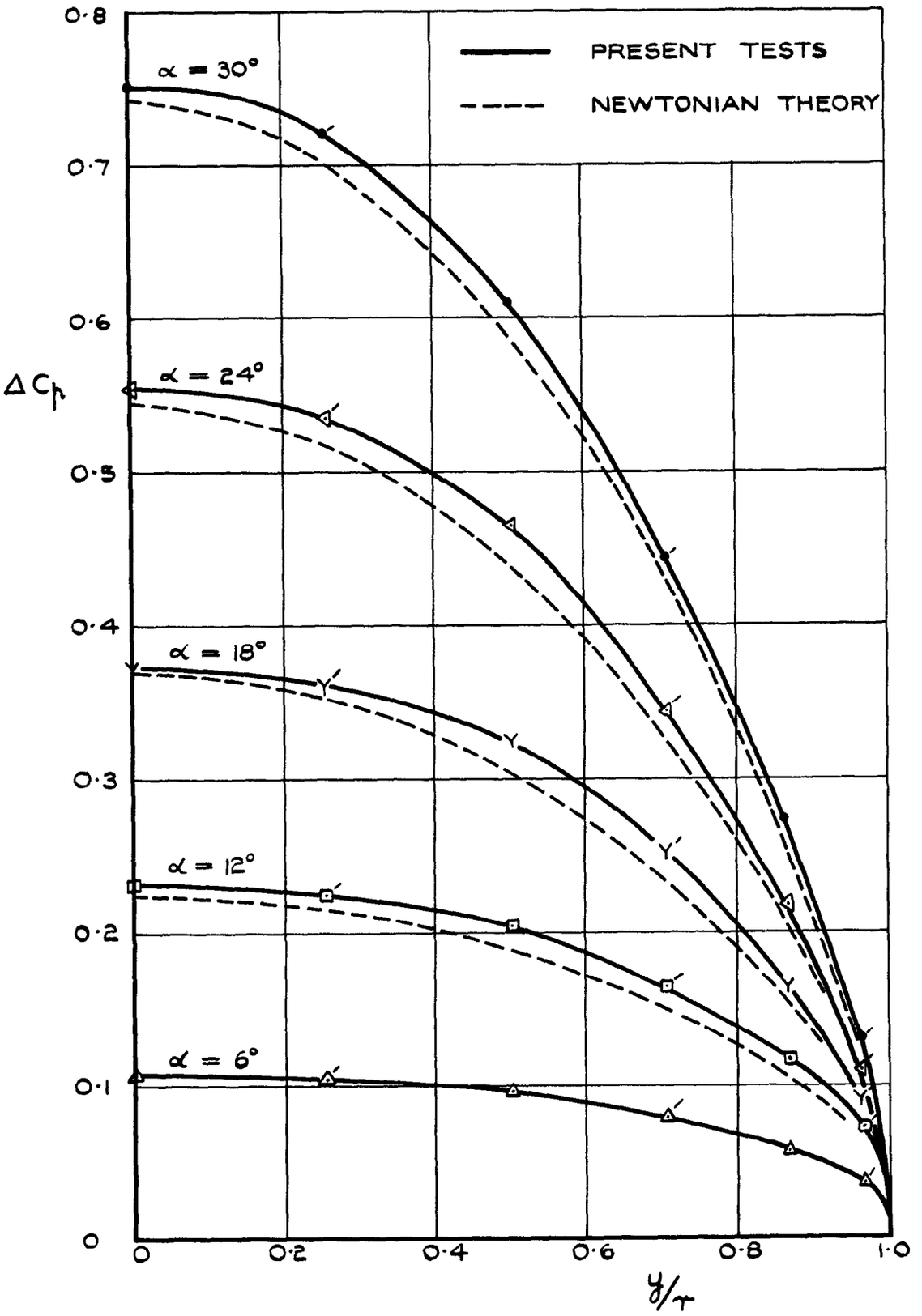

FIG. 9. DERIVATION OF LOCAL NORMAL FORCE COEFFICIENT $C_N(x)$ ON CONE FOREBODY AT $\frac{x}{\ell}=0.328$

$$C_N(x) = \int_0^{'} \Delta C_p \, d\left(\frac{y}{r}\right) \quad \text{WHERE} \quad \Delta C_p = (C_p)_\varphi - (C_p)_{\pi-\varphi}$$

FLAGGED SYMBOLS DENOTE VALUES INTERPOLATED FROM FIG. 5.

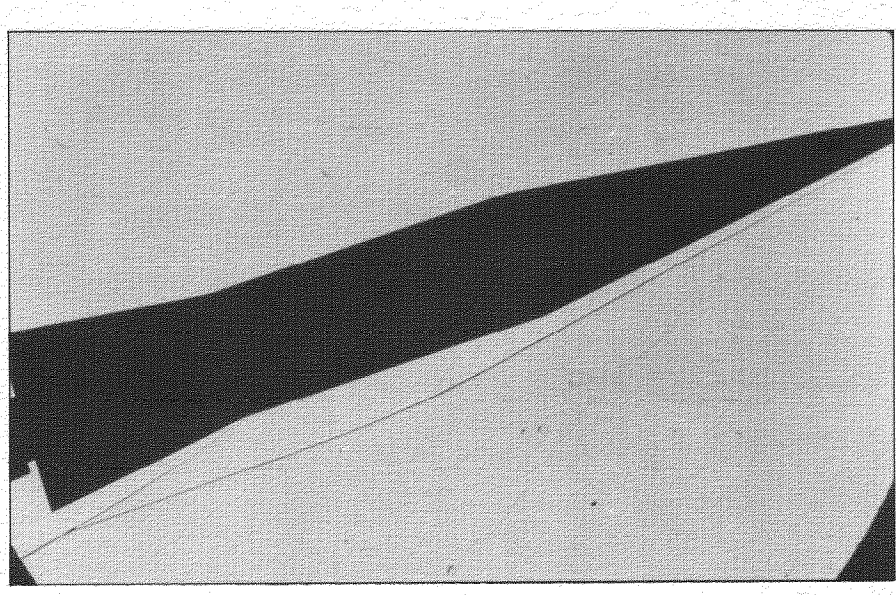

$\alpha = 18°$

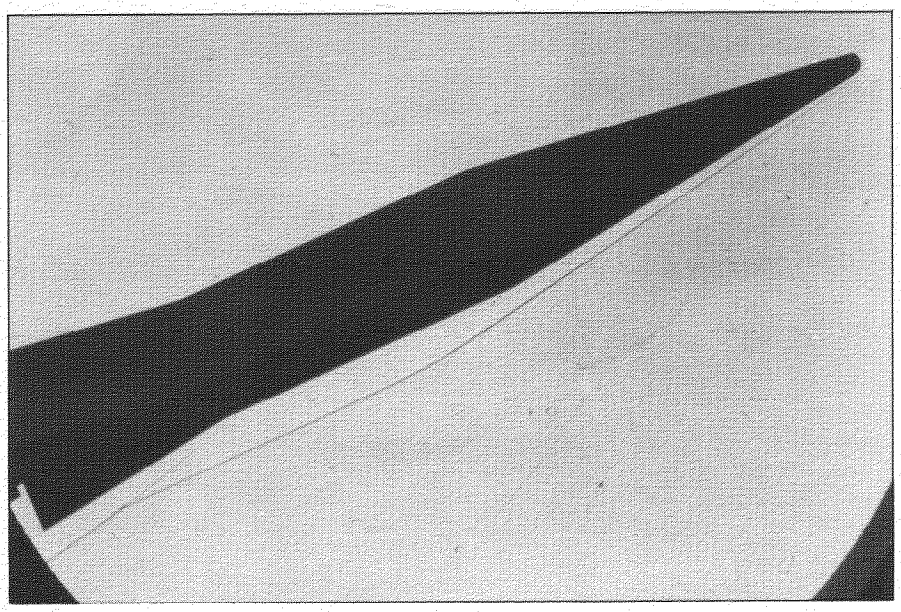

$\alpha = 24°$

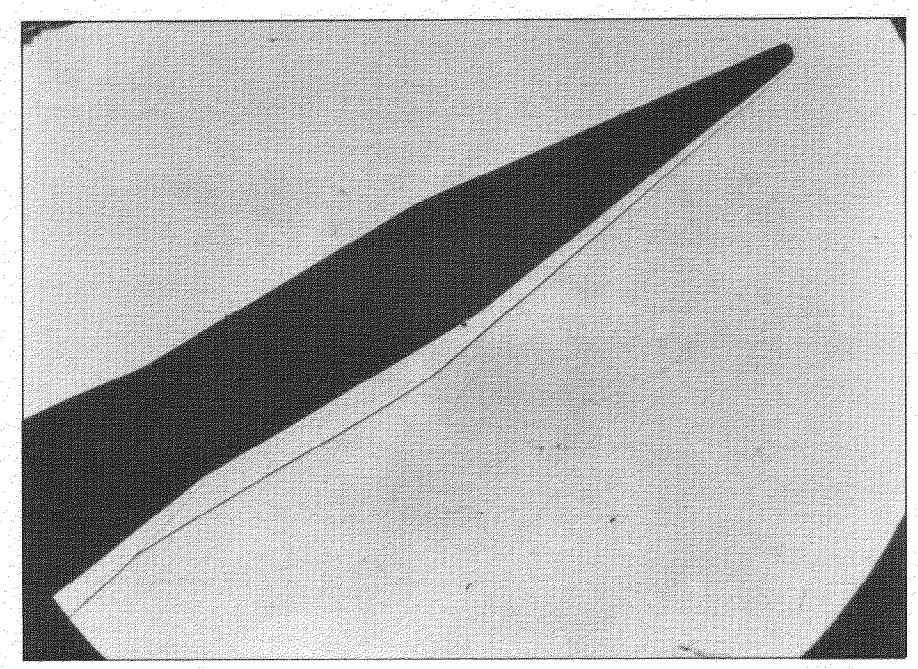

$\alpha = 30°$

A.R.C. C.P. No.657

533.696.3/.4 :
533.696.8 :
533.6.011.55 :
533.6.013.1 :
533.6.048.2

PRESSURE MEASUREMENTS ON A CONE-CYLINDER-FLARE CONFIGURATION AT M = 6.85 AND INCIDENCES UP TO 30°.

Peckham, D.H. January, 1962.

Pressure and force measurements were made on a slender cone-cylinder-flare configuration, slightly blunted at the nose, over an incidence range of 0° to 30° at a Mach number of 6.85.

Although force measurements showed good agreement with Newtonian theory, examination of local pressure distributions revealed considerable departures from theory. Thus it appears that the agreement of force measurements with theory was largely fortuitous, the local errors being self-compensating.

A.R.C. C.P. No.657

533.696.3/.4 :
533.696.8 :
533.6.011.55 :
533.6.013.1 :
533.6.048.2

PRESSURE MEASUREMENTS ON A CONE-CYLINDER-FLARE CONFIGURATION AT M = 6.85 AND INCIDENCES UP TO 30°.

Peckham, D.H. January, 1962.

Pressure and force measurements were made on a slender cone-cylinder-flare configuration, slightly blunted at the nose, over an incidence range of 0° to 30° at a Mach number of 6.85.

Although force measurements showed good agreement with Newtonian theory, examination of local pressure distributions revealed considerable departures from theory. Thus it appears that the agreement of force measurements with theory was largely fortuitous, the local errors being self-compensating.

A.R.C. C.P. No.657

533.696.3/.4 :
533.696.8 :
533.6.011.55 :
533.6.013.1 :
533.6.048.2

PRESSURE MEASUREMENTS ON A CONE-CYLINDER-FLARE CONFIGURATION AT M = 6.85 AND INCIDENCES UP TO 30°.

Peckham, D.H. January, 1962.

Pressure and force measurements were made on a slender cone-cylinder-flare configuration, slightly blunted at the nose, over an incidence range of 0° to 30° at a Mach number of 6.85.

Although force measurements showed good agreement with Newtonian theory, examination of local pressure distributions revealed considerable departures from theory. Thus it appears that the agreement of force measurements with theory was largely fortuitous, the local errors being self-compensating.

Published by
HER MAJESTY'S STATIONERY OFFICE

To be purchased from
York House, Kingsway, London W.C.2
423 Oxford Street, London W.1
13A Castle Street, Edinburgh 2
109 St. Mary Street, Cardiff
39 King Street, Manchester 2
50 Fairfax Street, Bristol 1
35 Smallbrook, Ringway, Birmingham 5
80 Chichester Street, Belfast 1
or through any bookseller

Printed in England

S.O. CODE No. 23-9013-57